RESEARCH ARTICLE

Spinocerebellar Ataxia Type 7 (SCA7): First Report of a Systematic Neuropathological Study of the Brain of a Patient with a Very Short Expanded CAG-Repeat

Rüb U[1]; Brunt ER[2]; Gierga K[1]; Seidel K[1]; Schultz C[1]; Schöls L[3]; Auburger G[4]; Heinsen H[5]; Ippel PF[6]; Glimmerveen WF[7]; Wittebol-Post D[8]; Arai K[9]; Deller T[1*]; de Vos RAI[10*]

[1] Institute for Clinical Neuroanatomy, and [4]Section Molecular Neurogenetics, Department of Neurology, J. W. Goethe University, Frankfurt/Main, Germany.
[2] University Medial Center Groningen, University of Groningen, The Netherlands.
[3] Center of Neurology and Hertie-Institute for Clinical Brain Research, University of Tübingen, Germany.
[5] Morphological Brain Research Unit, Julius Maximilians University, Würzburg, Germany.
[6] Department of Medical Genetics, and [8]F.C. Donders Institute of Ophthalmology, University Hospital Utrecht, The Netherlands.
[7] Department of Neurology, Ijsselmeer Ziekenhuizen, GA Emmeloord, The Netherlands.
[9] Department of Neurology, Chiba-East National Hospital, Chiba, Japan.
[10] Laboratorium Pathologie Oost Nederland, AD Enschede, The Netherlands.
[*] T. Deller and RAI de Vos are joint senior authors

Correspondence author:
Dr. Udo Rüb, Institute for Clinical Neuroanatomy, J. W. Goethe University, Theodor-Stern-Kai 7, D-60590 Frankfurt/Main, Germany
(E-mail: *U.Rueb@em.uni-frankfurt.de*)

Spinocerebellar ataxia type 7 (SCA7) represents a very rare and severe autosomal dominantly inherited cerebellar ataxia (ADCA). It belongs to the group of CAG-repeat or polyglutamine diseases with its underlying molecular genetical defect on chromosome 3p12-p21.1. Here, we performed a systematic study of the neuropathology on unconventional thick serial sections of the first available brain tissue of a genetically confirmed late-onset SCA7 patient with a very short CAG-repeat expansion. Along with myelin pallor of a variety of central nervous fiber tracts, we observed *i)* neurodegeneration in select areas of the cerebral cortex, and *ii)* widespread nerve cell loss in the cerebellum, thalamus, nuclei of the basal ganglia, and brainstem. In addition, upon immunocytochemical analysis using the anti-polyglutamine antibody 1C2, immunopositive neuronal intranuclear inclusions bodies (NI) were observed in all cerebellar regions, in all parts of the cerebral cortex, and in telencephalic and brainstem nuclei, irrespective of whether they underwent neurodegeneration. These novel findings provide explanations for a variety of clinical symptoms and paraclinical findings of both our and other SCA7 patients. Finally, our immunocytochemical analysis confirms previous studies which described the presence of NI in obviously degenerated brain and retinal regions as well as in apparently well-preserved brain regions and retina of SCA7 patients.

Brain Pathol 2005;15:287-295.

INTRODUCTION

Spinocerebellar ataxia type 7 (SCA7) is a very rare, severe and genetically defined autosomal dominant cerebellar ataxia (ADCA), accounts for 1% to 11% of genetically diagnosed ADCAs in diverse populations, corresponds to the progressive ADCA type II and may be associated with a retinal degeneration (6, 12, 15-17, 22, 25, 26, 29, 35, 45). Based on its underlying molecular genetic defect, SCA7 is assigned to the group of CAG-repeat or polyglutamine diseases whose currently known members share expanded, coding and meiotic unstable (CAG_n) trinucleotide repeats at specific gene loci (16, 22, 25, 26, 45, 46). The SCA7 gene has been mapped on chromosome 3p12-p21.1, encodes the disease protein designated ataxin-7, and in healthy individuals contains repeat sequences of 4 to 35 CAG triplets. In SCA7 patients and at-risk carriers it is expanded to approximately 38 to 70 CAG-repeats, while owing to its pronounced meiotic instability may show expansions of even up to 460 CAG-repeats (3, 6, 12, 15-17, 26, 29, 35). Though widely expressed in the central nervous system, retina, and in a variety of peripheral tissues, the normal form of ataxin-7 is found predominantly neuronal within the central nervous system and retina and localized to the cytoplasmic compartment, whereas the mutated form of ataxin-7 is restricted to neuronal nuclei, where it tends to aggregate into nuclear inclusions (NI) (3, 12, 16, 26, 29, 34, 35, 45). CAG-repeat expansions of approximately 60 and more commonly are associated with early onset and rapid progression of SCA7, present with the initial disease symptoms of visual impairments alone or in combination with ataxic symptoms, and commonly lead to blindness caused by degeneration of the retina. In contrast, patients with less than 60 expanded CAG-repeats in the mutated allele suffer from late SCA7 onset and first clinically exhibit ataxic symptoms, which may be followed by a progressive visual impairment (16, 25, 29, 33).

Although very few brains from patients who experienced early disease-onset and had long CAG-repeat expansions have been studied according to routine neuropathological procedures (3, 12, 22, 45), the current literature assumes that SCA7 may be associated with olivopontocerebellar atrophy (OPCA), retinal degeneration, involvement of the pallidum, substantia nigra, red nucleus, lateral geniculate body of the thalamus, spinal cord, and atrophy of the spinocerebellar tracts and cerebellar peduncles (3, 12, 22, 26, 35, 45). Here, we present the results of an initial systematic study of the neuropathology performed on the first available brain tissue of a genetically confirmed late-onset SCA7 patient.

Age (years)	Clinical and paraclinical findings
50	Disease onset with disequilibrium, gait and stance ataxia.
57	Gait and stance ataxia, mild ataxia of the upper and lower limbs, increased stretch reflexes in the upper and lower limbs, decreased sense of vibration in the lower limbs.
59	Additional dysarthria, repeated falls, dysmetrical horizontal saccades, saccadic smooth pursuits. Brain CT: Slight atrophy of the cerebellar vermis
60	Use of a walking cane
62	Use of a walker; later use of a wheelchair. Severe upper and lower limb ataxia, progressive problems with writing, beginning muscle atrophy.
72	Funduscopy: Retinal dystrophy not present.
73	Dependence on nursing care.
76	Patient is bedridden and unable to feed herself due to emerging dysphagia.
77	Death in a poor state of general and nutritive health as a result of a recurrent pulmonary infection and heart failure

Table 1. Summary of the clinical course of the SCA7 patient.

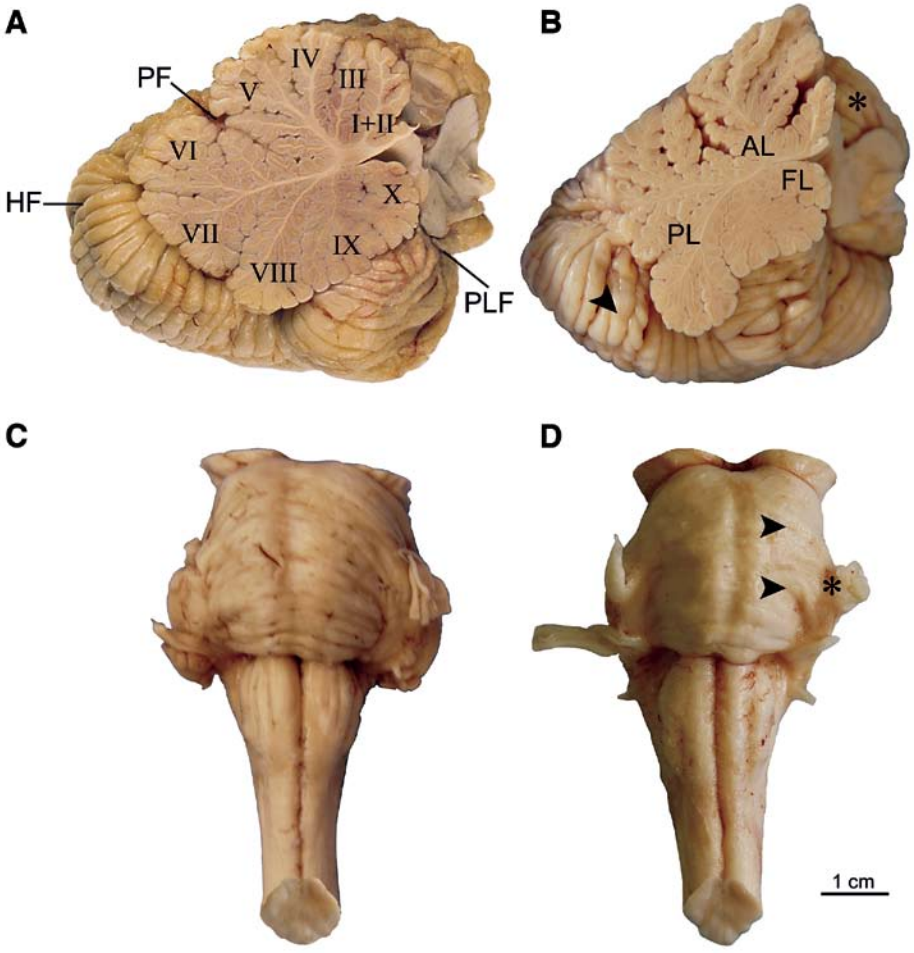

Figure 1. The cerebellum and lower brainstem. **A.** Paramedian aspect of the right cerebellum of a representative 50-year-old male control individual in comparison to that of (**B**) the SCA7 patient. Note the remarkable width of the primary fissure (PF), atrophy of lobules I-VII, as well as of the hemispheres of the anterior (AL, asterisk) and posterior lobes (PL, arrowhead), and the cerebellar tonsil (arrow). **C**. Anterior aspect of the pons and medulla oblongata of a representative 74-year-old male control individual in comparison to (**D**) that of the SCA7 patient, which showed an atrophy of the pons with loss of traversing pontocerebellar fibers (arrowheads) and reduction of the medial cerebellar peduncle (asterisk). Scale bar is valid for **A-D**. (Abbreviations: AL – Anterior lobe: I, II, III – Lobules I, II, III = Lingula and central lobule; IV, V – Lobules IV, V = Culmen; PL – Posterior lobe: VI – Lobule VI = Declive; VII – Lobule VII = Tuber and folium; VIII – Lobule VIII = Pyramis; IX – Lobule IX = Uvula; FL – Flocculonodular lobe: X – Lobule X = Nodule; HF – Horizontal fissure; PF – Primary fissure; PLF – Posterolateral fissure).

PATIENT AND METHODS

In the present investigation the brain of a clinically diagnosed 77-year-old female SCA7 patient along with the brains from 6 individuals without medical histories of neuropsychiatric diseases (3 females, 3 males; mean age at death 68.7 ± 10.4 years) were studied. The examination of these brains was approved by the Ethical board of the Faculty of Medicine at the J. W. Goethe University of Frankfurt/Main.

The 77-year-old female patient descended from a well-known autosomal dominant cerebellar ataxia type II (ADCA II) family in the northern region of the Netherlands. In 1997 when the patient was 70-years-old, the clinical diagnosis ADCA type II was confirmed genetically with the demonstration of 10 CAG-repeats in the normal and 39 copies in the mutated SCA7 gene on chromosome 3p12-p21.1 (15, 17). Her clinical course is summarized in Table 1.

An autopsy was performed in the SCA7 patient within 15 hours postmortem and in the control cases within 16.5 ± 2.5 hours. Subsequent to the fixation of the brains, spinal cords and the eyes in a 4% aqueous formaldehyde solution, the brainstems together with the cerebella of the SCA7 patient and the control individuals were cut perpendicular to the long axis of the brainstem at the level of the inferior colliculus. Thereafter the cerebella were removed from the brainstems by sagittal sections through the cerebellar peduncles. For purposes of routine neuropathological examination (performed by RAI de V), the following tissue blocks were embedded in paraffin: *i)* 24 tissue blocks from the left cerebral hemisphere and midbrain, *ii)* 12 tissue blocks from the spinal cord, as well as *iii)* 10 tissue blocks from the left cerebellum. The cerebral tissue blocks were cut into 6-µm thick frontal sections, the spinal tissue blocks into 6-µm thick horizontal sections and the cerebellar tissue blocks into 6-µm thick sagittal sections. At least 4 representative sections from each tissue block were immunostained either for α-synuclein, calbindin, glial fibrillary acidic protein, neurofilament, synaptophysin, ubiquitin, or the hyperphosphorylated form of the cytoskeletal protein tau and counterstained with hematoxylin, or only stained with hematoxylin and eosin (H&E). In addition, at least 4 representative conventional thick tissue sections from each block were immu-

nostained for the mutated form of human ataxin-7 with a polyclonal anti-ataxin-7 antibody (1: 2000; gift from Prof. C. van Broeckhoven; see Acknowledgments) (34) and counterstained with hematoxylin.

Finally, after paraffin embedding of the left eye of the SCA7 patient, it was cut into a complete series of conventional 4-µm thick horizontal sections. Three representative sections through the eye containing the optic nerve and the retina were either stained with H&E, or immunolabeled for the mutated human ataxin-7 (1:2000; gift from Prof C. van Broeckhoven; see Acknowledgments) and counterstained with hematoxylin (34).

The right cerebral hemispheres, right cerebella, as well as the brainstems of the SCA7 patient and control individuals were embedded in polyethylene glycol (PEG 1000, Merck, Darmstadt, Germany) (44). The cerebral tissue blocks were cut into uninterrupted series of 100-µm thick frontal sections, the cerebellar tissue blocks into uninterrupted series of 100-µm thick sagittal sections, and brainstem tissue blocks into uninterrupted series of 100-µm thick horizontal sections. A collection of the first, 11th, 21st, etc, of these 100-µm thick cerebral, cerebellar and brainstem sections were stained for lipofuscin pigment (aldehyde-fuchsin) and Nissl material (Darrow red) (10, 41, 43) and employed for the neuroanatomical delineation (8, 27, 37-39, 50) and assessment of neurodegeneration in the SCA7 patient. The second, 12th, 22nd, etc, serial cerebral, cerebellar and brainstem sections of the SCA7 patient and control individuals were processed according to a modified Heidenhain procedure to evaluate the structural integrity and myelinization of the central nervous fiber tracts (23, 39). Furthermore, in the SCA7 patient and all control individuals, a collection of the third, 13th, 23rd, etc, of the cerebral, cerebellar and brainstem serial sections was treated with a rabbit polyclonal antibody against glial fibrillary acidic protein (GFAP) (1:500, Dako, Glostrup, Denmark) to visualize reactive astrocytes. Finally, in each instance the collection of the fourth, 14th, 24th, etc, of the unconventional 100-µm thick serial sections through the cerebral hemispheres, cerebella and brainstems were immunostained with the monoclonal mouse anti-polyglutamine antibody 1C2 (1:1000; Chemicon, Temecula, Calif). In contrast to the polyclonal anti-ataxin-7 antibody applied to conventional thin sections, this antibody is directed against antigenic regions of pathologically altered proteins containing expanded polyglutamine stretches (46, 47). The specificity of the immunostaining was analyzed by omission of the primary antibodies. For single immunostaining,

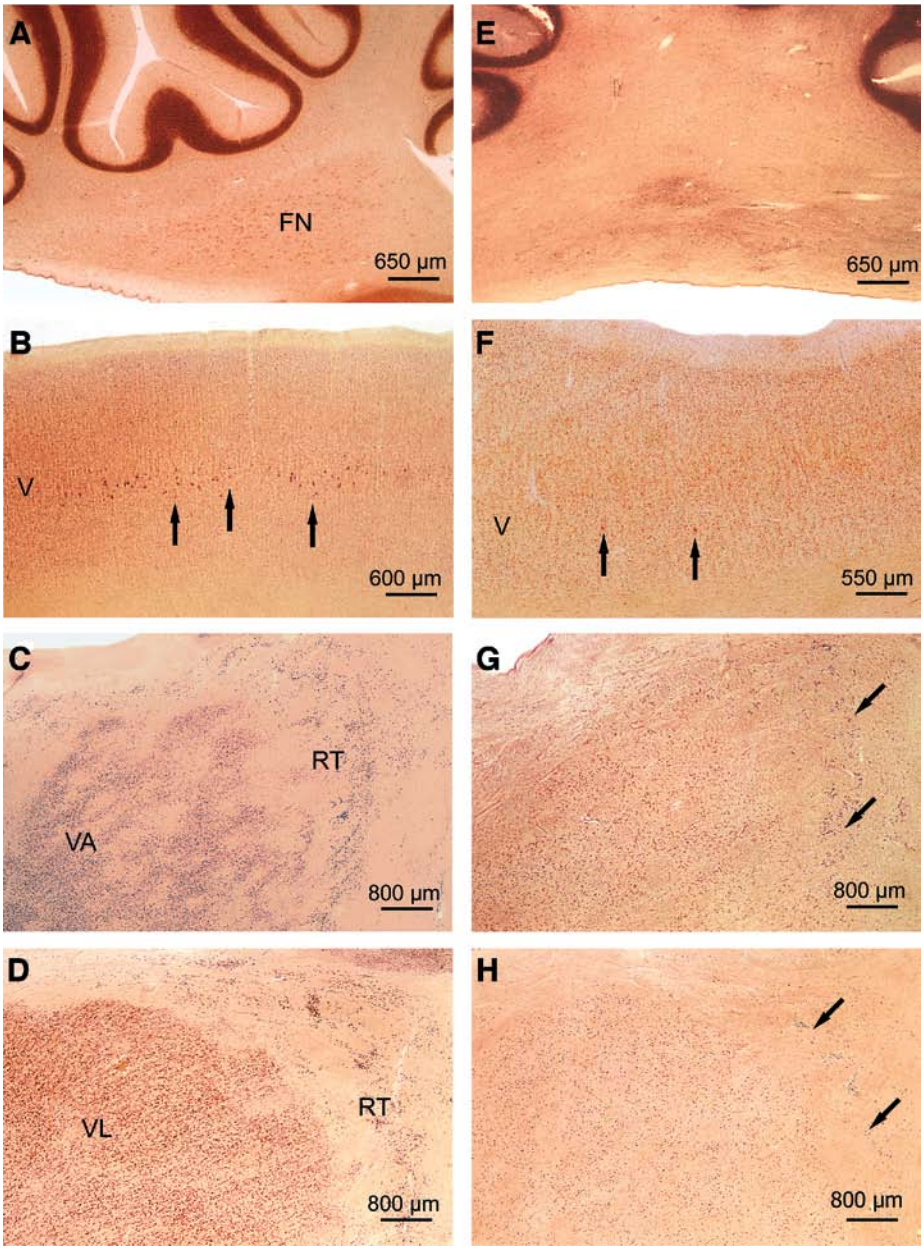

Figure 2. Deep cerebellar nuclei, primary motor cortex, and thalamus. **A.** Sagittal section through the right cerebellar hemisphere of a representative 65-year-old male control case without a previous medical history of neurological or psychiatric disease showing the fastigial nucleus (FN). **B.** Frontal section through the right cerebral hemisphere of a 75-year-old female control individual depicting the precentral gyrus with the primary motor cortex, which is characterized architectonically by *i)* the absence of an inner granular layer, and *ii)* the presence of giant pyramidal cells (ie, Betz cells) (arrows) in layer V (V). **C.** Frontal section through the extraterritorial reticular nucleus (RT) and the dorsolateral portion of the ventral anterior thalamic nucleus (VA) of a 79-year-old female control case without a medical history of neuropsychiatric diseases. **D.** Frontal section through the RT and dorsolateral portion of the ventral lateral thalamic nucleus (VL) of a representative 74-year-old male control individual. **E.** Severely degenerated FN of the 77-year-old female Dutch SCA7 patient. **F.** Considerable loss of giant pyramidal cells (ie, Betz cells) in the primary motor cortex of the SCA7 patient. Arrows indicate surviving giant pyramidal cells. **G.** Marked neurodegeneration in the VA and RT and (**H**) VL and RT of the Dutch SCA7 patient. Arrows point to remaining nerve cells (**A-H**: aldehyde-fuchsin Darrow red staining, 100-µm PEG sections). (Abbreviations: FN – Fastigial nucleus; RT – Reticular thalamic nucleus; VA – Ventral anterior thalamic nucleus; VL – Ventral lateral thalamic nucleus; V – Layer five of the primary motor cortex).

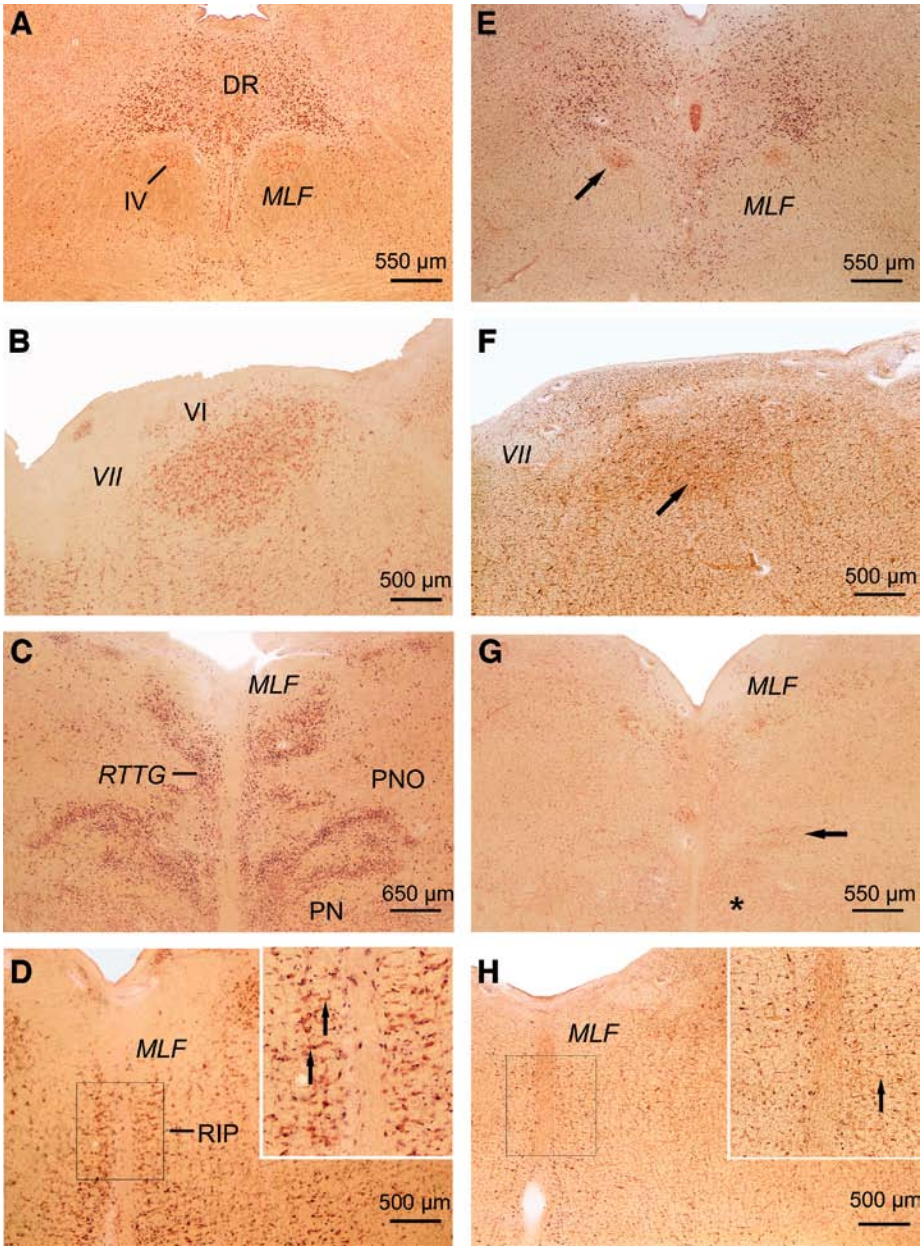

Figure 3. Oculomotor cranial nerve nuclei and premotor oculomotor nuclei. Horizontal section (**A**) through the caudal midbrain with the trochlear nucleus (IV) and (**B**) through the pontomedullary junction with the abducens nucleus (VI) of a representative 65-year-old male control case. **C.** Horizontal section through the rostral pons showing the reticulotegmental nucleus of the pons (RTTG, Nucleus of Bechterew) together with the pontine nuclei (PN) of a representative 69-year-old female control case. **D.** Horizontal section through the pontomedullary junction with the nucleus raphe interpositus (RIP) of a typical 65-year-old male control case. **E.** Obviously degenerated IV, (**F**) marked neuronal loss in the VI, (**G**) severely impaired RTTG and marked degeneration of the PN (asterisk), and (**H**) serious neurodegeneration in the RIP of the Dutch SCA7 patient. Framed areas in **D** and **H** are depicted at higher magnification at top right. Arrows in **E-H** point to remaining nerve cells. (**A-H**: aldehyde-fuchsin Darrow red staining, 100-µm PEG sections). (Abbreviations: DR – Dorsal raphe nucleus, supratrochlear part; PN – Pontine nuclei; PNO – Pontine reticular formation, oral nucleus; MLF – Medial longitudinal fascicle; RIP – Raphe interpositus nucleus; RTTG – Reticulotegmental nucleus of the pons (Bechterew); IV – Trochlear nucleus; VI – Abducens nucleus; VI – Abducens nerve; VII – Facial nerve).

incubation with the primary antibodies was performed for 12 hours at room temperature followed by incubation with biotinylated anti-mouse immunoglobulins for 1½ hours at room temperature. Bound antigens were visualized with the ABC-complex (Vectastain, Vector Laboratories, Burlingame, Calif) and 3,3-diaminobenzidine-tetra-HCl/H_2O_2 (DAB, D5637 Sigma, Taufkirchen, Germany). The extent of central nervous nerve cell loss, astrogliosis, and fiber loss and myelin pallor was qualitatively assessed in the SCA7 patient (none discernible 0, obvious +, severe ++). All investigations of unconventional thick sections including those immunostained with the 1C2 antibody were performed by UR.

RESULTS

Routine neuropathological findings. Routine neuropathological investigation revealed a markedly reduced brain weight of the SCA7 patient as compared to those of the control cases (1023 g versus 1336 ± 50.2 g). Reduction of the cerebellar white matter, atrophy of the vermal portion of the cerebellar lingula and central lobe, culmen, declive, tuber and folium, hemisphere of the anterior and posterior lobes, and cerebellar tonsil confirmed the findings of the previous neuroradiological examination (Figure 1A, B; Table 1). The brainstem exhibited atrophy of the pons with loss of traversing pontocerebellar fibers and reduction of the medial cerebellar peduncle (Figure 1C, D). Light microscopic investigation of conventional thin sections revealed: *i)* a marked atrophy of the cerebellar molecular and granular layers, severe and diffuse loss of the cerebellar Purkinje cells, most prominent in the central lobule, culmen, declive, tuber and folium of the vermis (Figure 4C, G); *ii)* considerable nerve cell loss and eosinophilic granular degeneration of the cerebellar dentate nucleus and a marked myelin pallor in its hilus; *iii)* neuronal loss and reactive astrogliosis in the substantia nigra, red nucleus, and internal and external segments of the pallidum; *iv)* severe myelin pallor of the dorsal columns, shrunken spinal cord motoneurons and destruction of the Clarke column in the thoracic part of the spinal cord; *v)* a slight concomitant Alzheimer disease (AD)-related cortical neurofibrillary pathology corresponding to Braak stage I (12); and *vi)* a chronic axonal neuropathy of the sural nerve. *vii)* Ataxin-7 immunoreactive neuronal nuclear inclusion bodies were present in the posterior cingulate gyrus, amygdala, putamen, caudate, and accumbens nuclei, as well as in the lateral geniculate body of the thalamus (Figure 4H).

Retinal findings. Microscopic examination of the conventional thin sections through the patient's retina showed aside from macular retinoschisis no additional

pathological alterations. A few intraneuronal ataxin-7 immunoreactive nuclear inclusions were detected in the outer nuclear layer of the retina (Figure 4D).

Findings of the systematic neuropathological study. The investigation of unconventionally thick Pigment-Nissl stained tissue sections confirmed all of the results of the routine neuropathological examination of the SCA7 patient's brain. However, in contrast to the routine neuropathological examination, we also found an affection of the deep cerebellar nuclei (Figure 2A, E), the cerebral cortex (Figure 2B, F), thalamus (Figure 2C, D, G, H), and basal ganglia nuclei (Table 2). In addition, in the patient's midbrain, pons and medulla oblongata a variety of limbic, somatomotor, oculomotor (Figure 3A-H), visceromotor, somatosensory, viscerosensory, auditory, vestibular, precerebellar, and reticular nuclei underwent neurodegeneration (Table 2).

In tissue sections stained for myelin, all of the SCA7 patient's fiber tracts related to the central optic system were well-preserved (Figure 4A, E). However, considerable myelin pallor and/or atrophy was present in a large number of central nervous commissural and projection fiber tracts, as well as in a subset of cranial nerves (Figure 4B, F; Table 3).

Substantial GFAP-immunopositive astrogliosis was found in a variety of the SCA7 patient's central nervous fiber tracts (Table 3) and in all central nervous gray components (Table 2) .

As opposed to the control cases, the unconventional thick central nervous tissue sections of the SCA7 patient showed an abundance of strongly 1C2-immunopositive neuronal intranuclear inclusions (NI). These NI not only were observed in surviving nerve cells of neurodegenerated CNS regions, but were present in nerve cells of all well-preserved central nervous regions (Table 2).

DISCUSSION

The present study represents a further step toward clarifying the extent of the pathological changes of SCA7, especially since it was performed on the first available brain tissue of a clinically diagnosed and genetically-confirmed SCA7 patient with a very short expansion of 39 CAG-repeats. As with other known late-onset

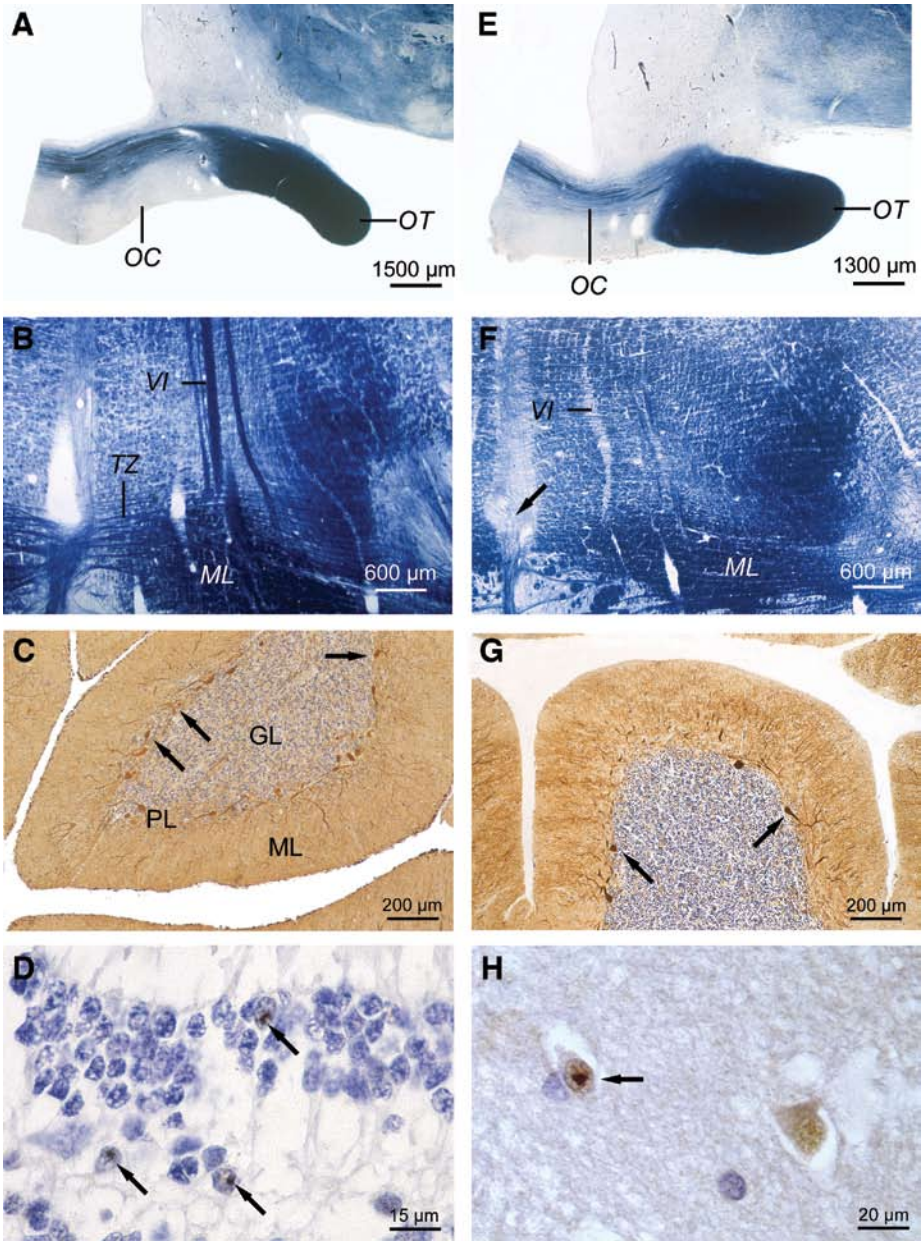

Figure 4. Fiber tracts and cytological findings. **A.** Frontal section through the basal forebrain at the level of the rostral pole of the thalamus with the optic chiasm (OC) and optic tract (OT) of a 79-year-old female control case without a medical history of neurological or psychiatric disease. **B.** Horizontal section through the pontomedullary junction of the same control individual depicting the abducens nerve (VI), the medial lemniscus (ML), and the crossing fibers of the trapezoid body (TZ). **C.** Sagittal section through the cortex of the cerebellar declive of a typical control individual showing the molecular (ML), Purkinje (PL) and granular (GL) cell layers. Arrows point to calbindin-immunopositive Purkinje cells. **D.** Ataxin-7-immunopositive intranuclear inclusion bodies (arrows) in surviving nerve cells of the outer nuclear layer of the retina in the SCA7 patient. **E.** Intact OC and OT of the SCA7 patient. **F.** Intact ML, atrophy and myelin pallor in the VI, and myelin pallor of the crossing fibers of the TZ (arrow) of the SCA7 patient. **G.** Marked loss of Purkinje cell bodies and dendrites in the cortex of the cerebellar declive of the SCA7 patient. Arrows point to surviving calbindin-immunopositive Purkinje cells. **H.** Ataxin-7-immunoreactive intranuclear inclusion body (arrow) in a surviving nerve cell of the posterior cingulate gyrus of the SCA7 patient. (**A**, **B**, **E**, **F**: modified Heidenhain staining, 100-µm PEG sections; **C**, **G**: Calbindin-immunostaining, counterstaining with hematoxylin, 6-µm paraffin sections; **D**: anti-ataxin-7 immunostaining, counterstaining with hematoxylin, 4-µm paraffin section; **H**: anti-ataxin-7 immunostaining, counterstaining with hematoxylin, 6-µm paraffin section). (Abbreviations: CU – Cuneate nucleus; CU – Cuneate fascicle; GR – Gracile nucleus; GR – Gracile fascicle; ML – Medial lemniscus; OC – Optic chiasm; OT – Optic tract; TZ – Trapezoid body; VI – Abducens nerve).

	NI	GFAP	Neuronal loss	N
Cerebellum	In all layers of the cerebellar cortex and in the deep nuclei	In all layers of the cerebellar cortex and in the deep nuclei	Purkinje cell layer	++
			Dentate nucleus	+
			Fastigial nucleus	++
Telencephalon	In all neo- and allocortical areas	In all neo- and allocortical areas	Entorhinal and transentorhinal cortices (pre-alpha layers)	+
			Primary motor cortex (Betz giant pyramidal cells)	+
	In all nuclei of the basal ganglia, basal forebrain, thalamus, habenula, hypothalamus, amygdala	In all nuclei of the basal ganglia, basal forebrain, thalamus, habenula, hypothalamus, amygdala	Reticular thalamic nucleus	+
			Fasciculosus thalamic nucleus	+
			Mediodorsal thalamic nucleus	++
			Ventral anterior thalamic nucleus	+
			Ventral lateral thalamic nucleus	+
			Ventral posterior lateral thalamic nucleus	
			Inferior and lateral subnuclei of the pulvinar	
			External and internal segments of the pallidum	
			Subthalamic nucleus	+
Midbrain	In all midbrain nuclei	In all midbrain nuclei	Rostral interstitial nucleus of the medial longitudinal fascicle	+
			Interstitial nucleus of Cajal	+
			Red nucleus	+
			Edinger-Westphal nucleus	+
			Oculomotor nucleus	+
			Substantia nigra	+
			Ventral tegmental area	+
			Pedunculopontine nucleus	+
			Trochlear nucleus	+
			Inferior colliculus	++
Pons	In all pontine nuclei	In all pontine nuclei	Sagulum	+
			Nuclei of the lateral lemniscus	++
			Pontine nuclei	+
			Reticulotegmental nucleus of the pons	++
			Pontine reticular formation	+
			Principal trigeminal nucleus	+
			Motor trigeminal nucleus	+
			Superior vestibular nucleus	++
			Abducens nucleus	+
			Facial nucleus	+
			Raphe interpositus nucleus	++
			Superior olive	+
			Lateral vestibular nucleus	++
			Interstitial vestibular nucleus	++
			Prepositus hypoglossal nucleus	+
			Medial vestibular nucleus	++
			Dorsal paramedian reticular nucleus	+
			Cochlear nuclei	+
			Vermiform nucleus	+

Table 2. Continued on next page.

SCA7 patients, our patient was not affected by disease-related impairments of the visual system (16, 22, 25, 29), shown here by absence of a retinal degeneration as normally found in SCA7 patients (29, 35).

During macroscopic investigation obvious gross abnormalities only were detected in the cerebellum and pons of our SCA7 patient. However, detailed neuropathological analysis of her brain revealed a more widespread telencephalic, cerebellar and brainstem lesional pattern than reported in the very rare previous postmortem studies, which were exclusively performed on brains from genetically confirmed early-onset SCA7 patients (3, 12, 22, 45). Among the central nervous lesions seen in our SCA7 patient, only the considerable neuronal loss in the pre-α layers of the transentorhinal and entorhinal regions may be attributable to a potential destructive effect of a slight

	NI	GFAP	Neuronal loss	N
Medulla oblongata	In all nuclei of the medulla oblongata	In all nuclei of the medulla oblongata	Arcuate nucleus	+
			Gigantocellular reticular nucleus	+
			Dorsal paragigantocellular reticular nucleus	+
			Spinal vestibular nucleus	++
			Ambiguus nucleus	+
			Inferior olive	+
			Conterminal nucleus	+
			Spinal trigeminal nucleus	+
			Hypoglossal nucleus	+
			Nucleus of Roller	+
			Lateral reticular nucleus	++
			External cuneate nucleus	+
			Cuneate nucleus	+
			Gracile nucleus	+
			Medial reticular nucleus	+
			Dorsal reticular nucleus	+

Table 2. Presence of neuronal intranuclear inclusion bodies (NI) and GFAP-immunopositive astrocytes (GFAP), and extent of central nervous neuronal loss in the SCA7 patient (N, neuronal loss; none discernible 0, obvious +, severe ++).

accompanying AD-related neurofibrillary pathology corresponding to stage I of the Braak staging system (9). Finally, in contrast to the hitherto reported genetically confirmed early-onset SCA7 patients (3, 22, 45), the visual pathway of our SCA7 patient, except for the presence of reactive astrocytes, displayed no noteworthy degenerative alterations. This may indicate that not only the clinical course of SCA7 (6, 12, 15, 16, 25, 29, 35) but also the extent of the underlying pathological process is triggered by the length of the expanded CAG-repeat sequence in the mutated SCA7 gene.

Our detailed neuropathological analysis was performed on unconventionally thick serial tissue through the right cerebral hemisphere and right cerebellum of the SCA7 patient and confirmed the results of the routine neuropathological examination of conventional paraffin sections through her left cerebral hemisphere and left cerebellum, but revealed additional obvious neurodegeneration in the cerebral cortex, deep cerebellar nuclei, thalamus and brainstem. These striking discrepancies demonstrate the superiority of the systematic neuropathological approach in comparison to the routine neuropathological approach in the field of basic pathoanatomical research (10, 41, 43).

In view of their known functional relevance, deterioration of distinct central nervous structures seen in our study can account for the presence of the following symptoms reported in our and other SCA7 patients: damage of *i)* giant Betz pyramidal cells in the primary motor cortex for pyramidal signs (2, 4, 15, 16, 22, 26, 29, 33, 35, 36, 50); *ii)* components of the cerebellothalamocortical circuits (pontine nuclei, cerebellar cortex and dentate nuclei, ventral lateral thalamic nucleus) and some of the precerebellar nuclei (arcuate, conterminal, dorsal paramedian reticular, external cuneate, lateral reticular, pontine, red, subventricular and vermiform nuclei, inferior olive) for the occurrence of ataxic symptoms and dysarthria (2, 4, 15, 16, 19, 26, 27, 29, 33, 35, 36, 45); *iii)* the pallidum, ventral anterior and mediodorsal thalamic nuclei for cognitive impairments (1, 6, 12, 15, 16, 25, 26, 29, 35, 43); *iv)* the peripheral nerves, ventral posterior lateral thalamic, gracile and cuneate nuclei for somatosensory deficits and pathologically altered somatosensory evoked potentials (13, 15, 16, 25, 28, 29, 32, 33, 45); *v)* the rostral interstitial nucleus of the medial longitudinal fascicle, interstitial nucleus of Cajal, and oculomotor and trochlear nuclei for slowing and palsy of vertical saccades (11, 20, 30, 31, 33, 36, 37, 45); *vi)* the Edinger-Westphal nucleus for impaired pupillary function (14, 20, 30); *vii)* the abducens nucleus for diplopia (20, 30, 31, 36); *viii)* the nucleus raphe interpositus for slow horizontal saccades (4, 29, 30, 33, 36, 37, 45); *ix)* the reticulotegmental nucleus of the pons and the cerebellar fastigial nucleus for saccadic smooth pursuits and dysmetrical saccades (24, 30, 33, 36, 42); *x)* the auditory brain stem nuclei (inferior colliculus, sagulum, nucleus of the lateral lemniscus, trapezoid nucleus, superior olive, dorsal and ventral cochlear nuclei) for auditory impairments and pathologically altered brainstem auditory evoked potentials (6, 7, 15, 16, 29, 33, 35, 45, 48); *xi)* the lateral vestibular nucleus for falls (5, 18, 33); *xii)* the facial nucleus for impairments of facial movements (6, 20, 29, 49); and *xiii)* the motor, principal and spinal trigeminal nuclei, and ambiguus, and hypoglossus nuclei for dysphagia (4, 16, 25, 26, 29, 33, 41, 45). Finally, in view of the integration of the inferior and lateral subnuclei of the pulvinar into neural circuits crucial for the generation of visual attention (21, 40), the superior and medial vestibular nuclei into the oculomotor circuits that subserve optokinetic nystagmus (11, 30) and vestibulo-ocular reaction (11, 30), as well as the role of the medial vestibular and prepositus hypoglossal nuclei in the pathogenesis of gaze-evoked nystagmus (11, 30, 31), their degeneration seen in the present study may suggest that visual attention deficits, impairments of optokinetic nystagmus, the vestibulo-ocular reaction and gaze-evoked nystagmus develop during the clinical course of SCA7.

Our study provides the first detailed analysis of the central nervous pattern neuronal intranuclear inclusions (NI) in SCA7, and confirms previous studies which described

	Affected white matter component	M	A+M	GFAP
Cerebellum	Cerebellar white matter	+	-	+
Telencephalon	Corpus callosum	+	-	+
	Anterior commissure	-	-	+
	Posterior commissure	-	-	+
	Fornix	-	-	+
	Corona radiata	-	-	+
	Internal capsule	-	-	+
	Extreme and external capsules	-	-	+
	Mamillothalamic tract	-	-	+
	Habenulointerpeduncular tract	-	-	+
	Triangular area of Wernicke	-	-	+
Midbrain	Cerebral peduncle	-	-	+
	Capsule of red nucleus	-	+	-
	Brachium of the inferior colliculus	-	-	-
	Oculomotor nerve	-	+	-
Pons	Lateral lemniscus	+	-	-
	Superior cerebellar peduncle	-	-	+
	Mesencephalic trigeminal tract	+	-	-
	Abducens nerve	-	+	-
	Trapezoid body	+	-	-
	Pontocerebellar fibers	-	+	-
	Medial cerebellar peduncle	-	-	+
	Inferior cerebellar peduncle	-	-	+
Medulla oblongata	Pyramidal tract	+	-	-
	Internal arcuate fibers	-	+	-
	Olivocerebellar fibers	-	+	-
	Cuneate fascicle	+	-	+
	Gracile fascicle	+	-	+
	Spinocerebellar tracts	+	-	-

Table 3. Extent of myelin pallor (M), atrophy and myelin pallor (A+M), as well as GFAP-immunopositive astrogliosis in the central nervous fiber tracts of the SCA7 patient (none discernible 0, obvious +, severe ++).

the presence of NI in obviously degenerated brain and retinal regions as well as in apparently well-preserved brain regions and retina of SCA7 patients (3, 12, 22, 26, 29, 34, 45). Owing to the presence of SCA7-related NI in affected as well as unaffected brain regions, as in other polyglutamine diseases, the precise role of NI in the pathogenesis of SCA7 is uncertain and it remains an open question whether these inclusions are pathogenic structures directly linked to the disease process underlying SCA7 (12, 29, 33).

ACKNOWLEDGMENTS

This study was supported by grants from the Deutsche Forschungsgemeinschaft (RU 1215/1-1), the Deutsche Heredo-Ataxie-Gesellschaft (DHAG), the ADCA-Vereniging Nederland and the Bernd Fink-Stiftung (Düsseldorf, Germany). The authors are grateful to Prof Christine van Broeckhoven (Laboratory of Neurogenetics, University of Antwerp, Antwerp, Belgium) for providing the anti-ataxin-7 antibody. The skillful assistance of M. Babl, E.D. Boswinkel-Kremers, O. Hampsink-Slotman, B. Meseck-Selchow, l. Rudnyeva, M. van Boekel (tissue processing and immunohistochemistry), M. Hütten (technical support) and Ms. I. Szász (graphics) is thankfully acknowledged. We thank J. Ironside (Department of Pathology, University of Edinburgh, United Kingdom) for his valuable comments and critical remarks.

REFERENCES

1. Alexander GE, Crutcher MD, DeLong MR (1990) Basal ganglia-thalamocortical circuits: Parallel substrates for motor, oculomotor, 'prefrontal' and 'limbic' functions. *Prog Brain Res* 85:119-146.

2. Alexander GE, DeLong NR (1992) Central mechanisms of initiation and control of movement. In: *Diseases of the Nervous System: Clinical Neurobiology*, 2nd Edition, Asbury AK, McKhann GM, McDonald WI (eds.), pp. 285-308, Saunders: Philadelphia.

3. Ansorge O, Giunti P, Michalik A, Van Broeckhoven C, Harding B, Wood N, Scaravilli F (2004) Ataxin-7 aggregation and ubiquitination in infantile SCA7 with 180 CAG repeats. *Ann Neurol* 56:448-452.

4. Bang OY, Lee Ph, Kim SS, Kim HJ, Huh K (2004) Pontine atrophy precedes cerebellar degeneration in spinocerebellar ataxia 7: MRI-based volumetric analysis. *J Neurol Neurosurg Psychiatry* 75:1452-1456.

5. Barmack NH (2003) Central vestibular system and posterior cerebellum. *Brain Res Bull* 60:511-541.

6. Benton CS, de Silva R, Rutledge SL, Bohlega S, Ashizawa T, Zoghbi HY (1998) Molecular and clinical studies in SCA-7 define a broad clinical spectrum and the infantile phenotype. *Neurology* 51:1081-1086.

7. Biacabe B, Chevallier JM, Avan P, Bonfils P (2001) Functional anatomy of auditory brainstem nuclei: application to the anatomical basis of brainstem auditory evoked potentials. *Auris Nasus Larynx* 28:85-94.

8. Braak H (1980) *Architectonics of the Human Telencephalic Cortex*, Springer: Berlin.

9. Braak H, Braak E (1991) Neuropathological stageing of Alzheimer-related changes. *Acta Neuropathol* 82:239-259.

10. Braak H, Rüb U, Del Tredici K (2003) Involvement of precerebellar nuclei in multiple system atrophy. *Neuropathol Appl Neurobiol* 29:60-76.

11. Büttner-Ennever JA, Büttner U (1992) Neuroanatomy of the ocular motor pathways. *Baillière's Clin Neurol* 1:263-287.

12. Cancel G, Duyckaerts C, Holmberg M, Zander C, Yvert G, Lebre AS, Ruberg M, Faucheux B, Agid Y, Hirsch E, Brice A (2000) Distribution of ataxin-7 in normal human brain and retina. *Brain* 12:2519-2530.

13. Chiappa KH (1997) *Evoked Potentials in Clinical Medicine*, 3rd Edition, Lippincott Williams & Wilkins Publishers: Philadelphia.

14. Corbett JJ, Thompson HS (1992) Pupillary function and dysfunction. In: *Diseases of the Nervous System: Clinical Neurobiology*, 2nd Edition, Asbury AK, McKhann GM, McDonald WI (eds.), pp. 490-500, Saunders: Philadelphia.

15. David G, Abbas N, Stevanin G, Dürr A, Yvert G, Cancel G, Weber C, Imbert G, Saudou F, Antoniou E, Drabkin H, Gemmill R, Giunti P, Benomar A, Wood N, Ruberg M, Agid Y, Mandel JL, Brice A (1997) Cloning of the SCA7 gene reveals a highly unstable CAG repeat expansion. *Nat Genet* 17:65-70.

16. David G, Dürr A, Stevanin G, Cancel G, Abbas N, Benomar A, Belal S, Lebre AS, Abada-Bendib M, Grid D, Holmberg M, Yahyaoui M, Hentati F, Chkili T, Agid Y, Brice A (1998) Molecular and clinical correlations in autosomal dominant cerebellar ataxia with progressive macular dystrophy (SCA7). *Hum Mol Genet* 7:165-170.

17. Del Favero J, Krols L, Michalik A, Theuns J, Lofgren A, Goossens D, Wehnert A, Van den Bossche D, Van Zand K, Backhovens H, van Regenmorter N, Martin JJ, Van Broeckhoven C (1998) Molecular genetic analysis of autosomal dominant cerebellar ataxia with retinal degeneration (ADCA type II) caused by CAG triplet repeat expansion. *Hum Mol Genet* 7:177-186.

18. Ghez C (1992) Posture. In: *Diseases of the Nervous System: Clinical Neurobiology*, 2nd Edition, Asbury AK, McKhann GM, McDonald WI (eds.), pp. 596-607, Saunders: Philadelphia.

19. Gilman S (1992) Cerebellum and motor dysfunction. In: *Diseases of the Nervous System: Clinical Neurobiology*, 2nd Edition, Asbury AK, McKhann GM, McDonald WI (eds.), pp. 368-389, Saunders: Philadelphia.

20. Gouw LG, Digre KB, Harris CP, Haines JH, Ptacek LJ (1994) Autosomal dominant cerebellar ataxia with retinal degeneration: clinical, neuropathologic, and genetic analysis of a large kindred. *Neurology* 44:1441-1447.

21. Grieve KL, Acuña C, Cudeiro J (2000) The primate pulvinar nuclei: vision and action. *Trends Neurosci* 23:35-39.

22. Holmberg M, Duyckaerts C, Dürr A, Cancel G, Gourfinkel-An I, Damier P, Faucheux B, Trottier Y, Hirsch EC, Agid Y, Brice A (1998) Spinocerebellar ataxia type 7 (SCA7): a neurodegenerative disorder with neuronal intranuclear inclusions. *Hum Mol Genet* 7:913-918.

23. Hutchins B, Weber JT (1983) A rapid myelin stain for frozen sections: modifications of the Heidenhain procedure. *J Neurosci Meth* 7:289-294.

24. Ilg UJ (1997) Slow eye movements. *Prog Neurobiol* 53:291-329.

25. Johansson J, Forsgren L, Sandgren O, Brice A, Holmgren G, Holmberg M (1998) Expanded CAG repeats in Swedish spinocerebellar ataxia type 7 (SCA7) patients: effect of CAG repeat length on the clinical manifestation. *Hum Mol Genet* 7:171-176.

26. Jonasson J, Strom AL, Hart P, Brannstrom T, Forsgren L, Holmberg M (2002) Expression of ataxin-7 in CNS and non-CNS tissue of normal and SCA7 individuals. *Acta Neuropathol* 104:29-37.

27. Jones EG (1985) *The Thalamus*, Plenum Press: New York.

28. Kaas JH (1990) Somatosensory system. In: *The Human Central Nervous System*, Paxinos G (ed.), pp. 813-844, Academic Press: San Diego.

29. Lebre AS, Brice A (2003) Spinocerebellar ataxia 7 (SCA7). *Cytogenet Genome Res* 100:154-163.

30. Leigh RJ, Zee DS (1991) *The Neurology of Eye Movements*, 2nd Edition, Davis Company, Philadelphia.

31. Leigh RJ, Zee DS (1992) Oculomotor control: normal and abnormal. In: *Diseases of the Nervous System: Clinical Neurobiology*, 2nd Edition, Asbury AK, McKhann GM, McDonald WI (eds.), pp. 368-389, Saunders: Philadelphia.

32. Lindblom U, Ochoa J (1992) Somatosensory function and dysfunction. In: *Diseases of the Nervous System: Clinical Neurobiology*, 2nd Edition, Asbury AK, McKhann GM, McDonald WI (eds.), pp. 213-228, Saunders: Philadelphia.

33. Martin J, Van Regemorter N, Del Favero J, Lofgren A, Van Broeckhoven C (1999) Spinocerebellar ataxia type 7 (SCA7)-correlations between phenotype and genotype in one large Belgian family. *J Neurol Sci* 168:37-46.

34. Mauger C, Del Favero J, Ceuterick C, Lubke U, Van Broeckhoven C, Martin J (1999) Identification and localization of ataxin-7 in brain and retina of a patient with cerebellar ataxia type II using antipeptide antibody. *Mol Brain Res* 74:35-43.

35. Michalik A, Martin JJ, Van Broeckhoven C (2004) Spinocerebellar ataxia type 7 associated with pigmentary retinal dystrophy. *Eur J Hum Genet* 12:2-15.

36. Oh AK, Jacobson KM, Jen JC, Baloh RW (2001) Slowing of voluntary and involuntary saccades: an early sign in spinocerebellar ataxia type 7. *Ann Neurol* 49:801-804.

37. Olszewski J, Baxter D (1982) *Cytoarchitecture of the Human Brain Stem*, 2nd Edition, Karger: Basel.

38. Paxinos G (1990) *The Human Central Nervous System*, Academic Press; San Diego.

39. Riley HA (1943) *An Atlas of the Basal Ganglia, Brainstem and Spinal Cord*, The Williams & Wilkins Company: Baltimore.

40. Robinson DL, Petersen SE (1992) The pulvinar and visual salience. *Trends Neurosci* 15:127-132.

41. Rüb U, Brunt ER, Del Turco D, de Vos RA, Gierga K, Paulson H, Braak H (2003) Guidelines for the pathoanatomical examination of the lower brain stem in ingestive and swallowing disorders and its application to a dysphagic spinocerebellar ataxia type 3 patient. *Neuropathol Appl Neurobiol* 29:1-13.

42. Rüb U, Bürk K, Schöls L, Brunt ER, de Vos RAI, Orozco Diaz G, Gierga K, Ghebremedhin E, Schultz C, Del Turco D, Mittelbronn M, Auburger G, Deller T, Braak H (2004) Damage to the reticulotegmental nucleus of the pons in spinocerebellar ataxia type 1, 2, and 3. *Neurology* 63:1258-1263.

43. Rüb U, Schultz C, Del Tredici K, Gierga K, Reifenberger G, de Vos RA, Seifried C, Braak H, Auburger G (2003) Anatomically-based guidelines for systematic investigations of the central somatosensory system and their application to a spinocerebellar ataxia type 2 (SCA2) patient. *Neuropath Appl Neurobiol* 29:418-433.

44. Smithson KG, MacVicar BA, Hatton GI (1983) Polyethylene glycol embedding: a technique compatible with immunocytochemistry, enzyme histochemistry, histofluorescence and intracellular staining. *Neurosci Methods* 7:27-41.

45. Takahashi J, Fujigasaki H, Zander C, El Hachimi KH, Stevanin G, Dürr A, Lebre AS, Yvert G, Trottier Y, The H, Hauw JJ, Duyckaerts C, Brice A (2002) Two populations of neuronal intranuclear inclusions in SCA7 differ in size and promyelocytic leukaemia protein content. *Brain* 125:1534-1543.

46. Trottier Y (2003) Antibody-based detection of CAG repeat expansion containing genes. *Methods Mol Biol* 217:83-89.

47. Trottier Y, Lutz Y, Stevanin G, Imbert G, Devys D, Cancel G, Saudou F, Weber C, David G, Tora L, Agid Y, Brice A, Mandel JL (1995) Polyglutamine expansion as a pathological epitope in Huntington's disease and four dominant cerebellar ataxias. *Nature* 378:403-406.

48. Webster WR, Garey LJ (1990) Auditory system. In: *The Human Central Nervous System*, Paxinos G (ed.), pp. 889-944, Academic Press: San Diego.

49. Yoritaka A, Tsukamoto T, Ohta K, Kishida S (2001) Facial myokymia associated with an isolated lesion of the facial nucleus. *Acta Neurol Scand* 104:182-184.

50. Zilles K (1990) Cortex. In: *The Human Central Nervous System*, Paxinos G (ed.), pp. 757-802, Academic Press: San Diego.